GEOPHYSICS, VOL. 71, NO. 2 (MARCH-APRIL 2006); P. T17–T30, 11 FIGS.
10.1190/1.2187792

Plane-wave propagation in attenuative transversely isotropic media

Yaping Zhu[1] and Ilya Tsvankin[1]

ABSTRACT

Directionally dependent attenuation in transversely isotropic (TI) media can influence significantly the body-wave amplitudes and distort the results of the AVO (amplitude variation with offset) analysis. Here, we develop a consistent analytic treatment of plane-wave properties for TI media with attenuation anisotropy. We use the concept of homogeneous wave propagation, assuming that in weakly attenuative media the real and imaginary parts of the wave vector are parallel to one another.

The anisotropic quality factor can be described by matrix elements Q_{ij}, defined as the ratios of the real and imaginary parts of the corresponding stiffness coefficients. To characterize TI attenuation, we follow the idea of the Thomsen notation for velocity anisotropy and replace the components Q_{ij} by two reference isotropic quantities and three dimensionless anisotropy parameters ϵ_Q, δ_Q, and γ_Q. The parameters ϵ_Q and γ_Q quantify the difference between the horizontal- and vertical-attenuation coefficients of P- and SH-waves, respectively, while δ_Q is defined through the second derivative of the P-wave attenuation coefficient in the symmetry direction. Although the definitions of ϵ_Q, δ_Q, and γ_Q are similar to those for the corresponding Thomsen parameters, the expression for δ_Q reflects the coupling between the attenuation and velocity anisotropy.

Assuming weak attenuation as well as weak velocity and attenuation anisotropy allows us to obtain simple attenuation coefficients linearized in the Thomsen-style parameters. The normalized attenuation coefficients for P- and SV-waves have the same form as the corresponding approximate phase-velocity functions, but both δ_Q and the effective SV-wave attenuation-anisotropy parameter σ_Q depend on the velocity-anisotropy parameters in addition to the elements Q_{ij}. The linearized approximations not only provide valuable analytic insight, but they also remain accurate for the practically important range of small and moderate anisotropy parameters — in particular, for near-vertical and near-horizontal propagation directions.

INTRODUCTION

Attenuation is a process that dissipates the energy of elastic waves and alters their amplitude and frequency content. The influence of attenuation on the amplitudes of reflected waves may cause errors in amplitude variation with offset (AVO) analysis. For example, Blangy (1994) speculates that some unexplained pitfalls in AVO interpretation may be attributed to attenuation-related phenomena. Reflection and transmission coefficients in isotropic attenuative media are discussed by Ursin and Stovas (2002) and, in transversely isotropic (TI) media, by Carcione (1997). More significant distortions of the AVO response, however, may be caused by the attenuation along the raypath of the reflected wave, in particular if the attenuation coefficient is angle dependent.

Physical-modeling experiments show that attenuation in anisotropic rocks can vary with direction, and the attenuation anisotropy is sometimes more significant than the velocity anisotropy (Hosten et al., 1987; Tao and King, 1990; Arts and Rasolofosaon, 1992). The same conclusion is drawn by Carcione (2000), who models wavefields propagating through attenuative shale models. Prasad and Nur (2003) observe P-wave attenuation anisotropy for reservoir rocks (such as fluvial sandstones and dolomites) by measuring the attenuation coefficient in two orthogonal directions. Their experiments indicate that the attenuation anisotropy can be related to the texture of sedimentary rocks.

For azimuthally anisotropic formations that contain systems of small-scale aligned fractures, both velocity and attenuation vary with azimuth. The azimuthal variation of the attenuation

Manuscript received by the Editor September 11, 2004; revised manuscript received July 5, 2005; published online March 9, 2006; publisher error corrected March 13, 2006.
[1]Colorado School of Mines, Center for Wave Phenomena, Department of Geophysics, 1500 Illinois St., Golden, Colorado 80401-1877. E-mail: yzhu@dix.mines.edu; ilya@dix.mines.edu.

coefficient can be used to estimate the orientation and some physical properties of the fractures (Rathore et al., 1995; Lynn et al., 1999; Chichinina et al., 2004).

Although the physical mechanism of intrinsic attenuation is not clearly understood, a number of parameters have been introduced to quantify attenuation-related amplitude decay (e.g., Johnston and Toksöz, 1981). The most common choices are the quality factor Q and the magnitude of the imaginary part of the complex wavenumber, usually called the attenuation coefficient. A detailed discussion of wave propagation in anisotropic attenuative media is given by Carcione (2001). His treatment, however, is based on the stiffness coefficients, and the results are not generally expressed in a form amenable to data-processing applications. As demonstrated below, analysis of the influence of anisotropic attenuation on seismic signatures can be facilitated by introducing dimensionless anisotropy parameters responsible for the angle-dependent quality factor.

The terminology in this paper is designed to clearly distinguish between the anisotropy of velocity and attenuation. To ensure consistency with existing literature on nonattenuative anisotropic media, terms such as *anisotropic media* or *transversely isotropic (TI) media* refer to the velocity anisotropy. When discussing attenuative media, we explicitly specify the character of the attenuation. For example, the terms *TI medium with isotropic attenuation* means that the model is transversely isotropic with respect to the velocity function, but the attenuation is isotropic (i.e., independent of direction).

For plane waves propagating through attenuative media, the orientations of the real and the imaginary parts of the wave vector are generally different from one another. This means that the planes of constant phase and constant amplitude do not coincide (Borcherdt and Wennerberg, 1985; Borcherdt et al., 1986; Krebes and Slawinski, 1991; Krebes and Le, 1994), and the direction of wave propagation deviates from the direction of maximum attenuation. However, when the wavefield is excited by a point source in a weakly attenuative homogeneous medium, the angle between the real and imaginary parts of the wave vector (the so-called *inhomogeneity angle*) is usually small, and the rate of attenuation is highest close to the propagation direction (Ben-Menahem and Singh, 1981; I. Pšenčík, 2004, personal communication). Here, we show that as long as the sine of the inhomogeneity angle is of the same order as the velocity-anisotropy and attenuation-anisotropy parameters, the misalignment of the real and imaginary parts of the wave vector has negligible influence on the attenuation coefficient. Therefore, in most of the discussion the real and imaginary parts of the wave vector are taken to be parallel to one another, which corresponds to the homogeneous wave-propagation.

This paper is devoted to plane-wave signatures in TI media with both isotropic and TI attenuation. After defining the quality-factor elements Q_{ij} through the ratios of the real and imaginary parts of the stiffness coefficients, we introduce Thomsen-style parameters that describe the angle-dependent attenuation. The advantages of this notation are demonstrated by analyzing the attenuation coefficient as a function of phase angle. To gain insight into the behavior of the attenuation coefficients for P- and SV-waves, we simplify the exact equations under the assumptions that the attenuation and velocity anisotropy, as well as the attenuation itself, are weak. The accuracy of the approximate attenuation coefficients is verified by numerical tests for representative TI models.

DEFINITION OF THE Q MATRIX

The quality factor Q can be related to several other parameters used in attenuation measurements, such as the attenuation coefficient, logarithmic decrement of amplitude, and complex modulus (Johnston and Toksöz, 1981). All of those parameters, however, were originally designed for isotropic attenuation and need to be generalized for anisotropic materials.

To develop a consistent description of the Q-factor for both isotropic and anisotropic attenuation, we follow Carcione (2001, p. 58) in defining Q as twice the time-averaged strain-energy density divided by the time-averaged dissipated-energy density. In terms of the complex stiffness coefficients, the Q-factor matrix is given by

$$Q_{ij} \equiv \frac{c_{ij}}{c^I_{ij}}, \tag{1}$$

where c_{ij} and c^I_{ij} are the real and the imaginary parts, respectively, of the stiffness coefficient $\tilde{c}_{ij} = c_{ij} + i c^I_{ij}$. Note there is no summation over i or j in equation 1.

Our analysis is restricted to TI media with either isotropic or TI attenuation. The symmetry axis is assumed to be vertical (VTI), but because all results are derived for a homogeneous medium, they can be readily adapted to TI models with any symmetry-axis orientation.

As follows from equation 1, the **Q** matrix inherits the structure of the stiffness matrix. For the case of VTI media with VTI attenuation, the matrices c_{ij} and c^I_{ij} have the same VTI symmetry, and the **Q** matrix has the form

$$\mathbf{Q} = \begin{bmatrix} Q_{11} & Q_{12} & Q_{13} & 0 & 0 & 0 \\ Q_{12} & Q_{11} & Q_{13} & 0 & 0 & 0 \\ Q_{13} & Q_{13} & Q_{33} & 0 & 0 & 0 \\ 0 & 0 & 0 & Q_{55} & 0 & 0 \\ 0 & 0 & 0 & 0 & Q_{55} & 0 \\ 0 & 0 & 0 & 0 & 0 & Q_{66} \end{bmatrix}, \tag{2}$$

where

$$Q_{12} = Q_{11} \frac{c_{11} - 2c_{66}}{c_{11} - 2c_{66}\dfrac{Q_{11}}{Q_{66}}}.$$

When both the real and imaginary parts of the stiffness matrix have isotropic structure, the Q-factor is described by only two independent parameters, Q_{33} and Q_{55}:

$$\mathbf{Q} = \begin{bmatrix} Q_{33} & Q_{13} & Q_{13} & 0 & 0 & 0 \\ Q_{13} & Q_{33} & Q_{13} & 0 & 0 & 0 \\ Q_{13} & Q_{13} & Q_{33} & 0 & 0 & 0 \\ 0 & 0 & 0 & Q_{55} & 0 & 0 \\ 0 & 0 & 0 & 0 & Q_{55} & 0 \\ 0 & 0 & 0 & 0 & 0 & Q_{55} \end{bmatrix}. \tag{3}$$

The component $Q_{13} = Q_{12}$ can be obtained from Q_{33} and Q_{55} as

$$Q_{13} = Q_{33}\frac{c_{33} - 2c_{55}}{c_{33} - 2c_{55}\dfrac{Q_{33}}{Q_{55}}}.$$

The P-wave attenuation is controlled by Q_{33}, while Q_{55} is responsible for the SV-wave attenuation.

According to the attenuation measurements in sandstones by Gautam et al. (2003), the Q-factor for P-waves may be either larger or smaller than that for SV-waves, depending on the mobility of fluids in the rock. The crossover frequency, for which $Q_{33} = Q_{55}$, corresponds to the special case when all components of the **Q** matrix are identical:

$$Q_{ij} = Q. \tag{4}$$

If the quality factor is given by equation 4, the attenuation for both P- and S-waves is isotropic (independent of direction), even for arbitrarily anisotropic media.

Anisotropic attenuation can be described by calculating the so-called eigenstiffnesses from the c_{ij} matrix and applying relaxation functions to the eigenstiffnesses to obtain the complex stiffness coefficients $\tilde{c}_{ij}$ and the **Q** matrix (Helbig, 1994). For TI media, those operations are detailed by Carcione (2001). Here, we do not consider any specific attenuation mechanism and focus on examining wave propagation for the general TI structure of the **Q** matrix.

The discussion below is based on the assumption of a frequency-independent Q, which is often valid in the seismic-frequency band. In a more rigorous description of attenuation, the complex stiffness components and the Q-factor vary with frequency, as does the velocity. Our results, however, can still be applied for any given frequency, and the Thomsen-style anisotropy coefficients become frequency dependent.

Christoffel equation for anisotropic, attenuative media

The displacement of a harmonic plane wave can be written as

$$\tilde{\mathbf{u}} = \tilde{\mathbf{U}}\exp[i(\omega t - \tilde{\mathbf{k}}\cdot\mathbf{x})], \tag{5}$$

where $\tilde{\mathbf{U}}$ denotes the polarization vector, ω is the angular frequency, t is the time, and $\tilde{\mathbf{k}}$ is the wave vector that becomes complex in the presence of attenuation: $\tilde{\mathbf{k}} = \mathbf{k} - i\mathbf{k}^I$. The imaginary part ($\mathbf{k}^I$) of the wave vector is sometimes called the attenuation vector. In general, $\mathbf{k}^I$ is not parallel to $\mathbf{k}$, which means that the planes of constant phase and constant amplitude do not coincide and the direction of the fastest amplitude decay deviates from the phase-velocity vector. Then wave propagation is called inhomogeneous, and the angle between $\mathbf{k}^I$ and $\mathbf{k}$ is called the inhomogeneity angle.

While the inhomogeneity angle is a free parameter in plane-wave propagation, for wavefields excited by point sources in weakly attenuative media, the deviation of $\mathbf{k}^I$ from $\mathbf{k}$ is usually small (Ben-Menahem and Singh, 1981). As discussed in Appendices A and B, if the sine of the inhomogeneity angle is of the same order as the velocity-anisotropy and attenuation-anisotropy parameters, the deviation of $\mathbf{k}^I$ from $\mathbf{k}$ has a negligibly small influence on both the attenuation coefficient and phase velocity. Hence, our treatment of plane waves is restricted to homogeneous wave-propagation, for which $\mathbf{k}$ and $\mathbf{k}^I$ are parallel to one another so that $\tilde{\mathbf{k}} = \mathbf{n}(k - ik^I)$, where $\mathbf{n}$ is the unit vector in the phase direction, $k = |\mathbf{k}|$, and $k^I = |\mathbf{k}^I|$.

By substituting the plane wave of equation 5 into the equation of motion, we obtain the Christoffel equation of the same form as in nonattenuative media:

$$[\tilde{G}_{ik} - \rho\tilde{V}^2\delta_{ik}]\tilde{U}_k = 0. \tag{6}$$

Here, $\tilde{G}_{ik} = \tilde{c}_{ijkl}n_j n_l$ is the Christoffel matrix that depends on the complex stiffnesses $\tilde{c}_{ijkl}$ and the phase direction $\mathbf{n}$, ρ is the density, δ_{ik} is Kronecker's delta, and $\tilde{V} = \omega/\tilde{k}$ is the complex phase velocity ($\tilde{k} = |\tilde{\mathbf{k}}|$). The real part V of the phase velocity is given by (Carcione, 2001) as

$$V = \left[\mathrm{Re}\left(\frac{1}{\tilde{V}}\right)\right]^{-1} = \frac{\omega}{k}. \tag{7}$$

Below, we examine the solutions of the Christoffel equation 6 for all three wave types (P, SV, SH) in VTI media with both isotropic and VTI attenuation.

SH-WAVE ATTENUATION

For waves propagating in the $[x_1, x_3]$-plane of VTI media, the Christoffel equation 6 splits into an equation for the SH-wave polarized in the x_2-direction and two coupled equations for the in-plane polarized P- and SV-waves. The equation for the wave vector of the SH-wave has the same form as that in nonattenuative media, but the stiffness coefficients and wavenumbers are complex quantities:

$$\tilde{c}_{66}\tilde{k}_1^2 + \tilde{c}_{55}\tilde{k}_3^2 - \rho\omega^2 = 0. \tag{8}$$

Isotropic attenuation

As shown in Appendix A for homogeneous wave-propagation in a medium with isotropic Q ($Q = Q_{55} = Q_{66}$), the imaginary part of equation 8 reduces to

$$\mathcal{K}_2 \equiv \frac{k^2 - (k^I)^2}{Q} - 2kk^I = 0. \tag{9}$$

The assumption of isotropic Q for SH-waves does not involve the condition $Q_{33} = Q_{55}$. Solving for k^I, we find [also see equation 2.122 in Carcione (2001)]

$$k^I = k\left(\sqrt{1 + Q^2} - Q\right). \tag{10}$$

It is convenient to introduce the normalized attenuation coefficient $\mathcal{A}$ that defines the rate of amplitude decay per wavelength:

$$\mathcal{A} \equiv \frac{k^I}{k}. \tag{11}$$

For brevity, the word *normalized* is omitted in most of the text below. Equation 10 shows that the coefficient $\mathcal{A}$ for SH-waves in media with isotropic Q is independent of the phase angle. When attenuation is weak (i.e., $1/Q \ll 1$), equation 10 yields

$$\mathcal{A}_{SH} = \frac{1}{2Q}. \tag{12}$$

The weak-attenuation approximation 12 is close to the exact attenuation coefficient $\mathcal{A}$ for the practically important range $Q > 10$ and breaks down only for strongly attenuative media (Figure 1).

The real part of the Christoffel equation 8 can be used to obtain the phase velocity of the SH-wave (Appendix A):

$$V_{SH}(\theta) = \xi_Q V_{SH}^{\text{elast}}(\theta), \tag{13}$$

where V_{SH}^{elast} is the SH-wave phase velocity in the reference nonattenuative medium (equation A-15) and ξ_Q is given in equation A-19. In the limit of weak attenuation, the phase velocity becomes

$$V_{SH}(\theta) = V_{SH}^{\text{elast}}(\theta)\left(1 + \frac{1}{2Q^2}\right). \tag{14}$$

For a realistic range of Q-values, the influence of attenuation on the real part of the wavenumber and therefore on the phase velocity can be ignored. Even for strongly attenuative media with $Q = 5$, the contribution of the term $1/2Q^2$ in equation 14 is limited to 2% of the velocity V_{SH}. Attenuation, however, causes velocity dispersion that is not always negligible, even in the seismic-frequency band.

VTI attenuation

Since the real and imaginary parts of the wave vector are coupled in the Christoffel equation, the directional dependence of the attenuation is influenced by the velocity anisotropy of the material. The physical reasons for the attenuation and velocity anisotropy in TI media may be similar. For example, preferential orientation of clay platelets in shales may be responsible not just for the velocity anisotropy (Sayers, 1994) but also for the attenuation anisotropy. Therefore, it is reasonable to assume that the symmetry of the attenuation in TI media is the same as that of the phase velocity. Furthermore, we take the symmetry axes of the attenuation coefficient and velocity function as parallel to one another, which results in the general VTI form of the **Q** matrix in equation 2.

The Christoffel equation 8 yields the following relationship between the real and the imaginary SH-wavenumbers (Appendix A):

$$k^2 - (k^I)^2 - 2Q_{55}\alpha k k^I = 0, \tag{15}$$

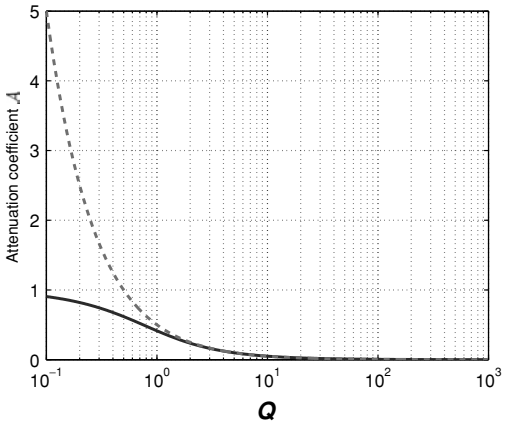

Figure 1. Normalized attenuation coefficient $\mathcal{A}$ for SH-waves as a function of the Q-factor for a medium with $Q_{55} = Q_{66} = Q$. The solid line is the exact $\mathcal{A}$ from equations 10 and 11; the dashed line is the weak-attenuation approximation 12.

where $\gamma \equiv (c_{66} - c_{55})/(2c_{55})$ is Thomsen's velocity-anisotropy parameter for SH-waves and

$$\alpha \equiv \frac{(1+2\gamma)\sin^2\theta + \cos^2\theta}{(1+2\gamma)\dfrac{Q_{55}}{Q_{66}}\sin^2\theta + \cos^2\theta}. \tag{16}$$

Equation 16 is essentially identical to equation 35 in Krebes and Le (1994). Solving equation 15 for k^I, we find the SH-wave-attenuation coefficient:

$$\mathcal{A}_{SH} \equiv \frac{k^I}{k} = \sqrt{1 + (Q_{55}\alpha)^2} - Q_{55}\alpha. \tag{17}$$

In the weak-attenuation limit, equation 17 reduces to

$$\mathcal{A}_{SH} = \frac{1}{2Q_{55}\alpha}. \tag{18}$$

Equation 18 shows that Q_{55} is multiplied with the directionally dependent parameter α to form the effective Q-factor for the SH-wave, $Q_{55}^{\text{eff}} = Q_{55}\alpha$. At vertical incidence ($\theta = 0^\circ$), $\alpha = 1$ and $\mathcal{A}_{SH} = 1/(2Q_{55})$. In the horizontal direction ($\theta = 90^\circ$), $\alpha = Q_{66}/Q_{55}$ and $\mathcal{A}_{SH} = 1/(2Q_{66})$. For intermediate propagation directions, α reflects the coupling between the SH-wave velocity-anisotropy parameter γ and the ratio of the elements Q_{55} and Q_{66}. The contribution of the ratio Q_{55}/Q_{66} in equation 16 is used below to define an attenuation-anisotropy parameter analogous to Thomsen's parameter γ.

P- AND SV-WAVE ATTENUATION

Because of the coupling between P- and SV-waves, the equations governing their velocity and attenuation are more complicated than those for SH-waves. While the complex wavenumbers for P- and SV-waves can be evaluated numerically from equations B-3 and B-4 in Appendix B, the expression for the imaginary wavenumber k^I is cumbersome. Therefore, we use approximate solutions to study the dependence of the attenuation coefficients of P- and SV-waves on the medium parameters.

If both the attenuation anisotropy and attenuation itself are weak, the coefficient $\mathcal{A}$ for both P- and SV-waves can be found as (see Appendix C)

$$\mathcal{A} = \frac{1}{2Q_{33}}(1 + \mathcal{H}), \tag{19}$$

where $\mathcal{H} \equiv \mathcal{H}_u/\mathcal{H}_d$,

$$\begin{aligned}\mathcal{H}_u \equiv{}& \left(c_{11}\sin^2\theta\frac{Q_{33}-Q_{11}}{Q_{11}} + c_{55}\cos^2\theta\frac{Q_{33}-Q_{55}}{Q_{55}}\right)\\ &\times (c_{55}\sin^2\theta + c_{33}\cos^2\theta - \rho V^2)\\ &+ c_{55}\sin^2\theta\frac{Q_{33}-Q_{55}}{Q_{55}}(c_{11}\sin^2\theta + c_{55}\cos^2\theta - \rho V^2)\\ &- 2\left(c_{13}\frac{Q_{33}-Q_{13}}{Q_{13}} + c_{55}\frac{Q_{33}-Q_{55}}{Q_{55}}\right)(c_{13}+c_{55})\\ &\times \sin^2\theta\cos^2\theta,\end{aligned} \tag{20}$$

and

$$\begin{aligned}\mathcal{H}_d \equiv{}& \rho V^2[(c_{55}+c_{11})\sin^2\theta\\ &+ (c_{33}+c_{55})\cos^2\theta - 2\rho V^2].\end{aligned} \tag{21}$$

The phase-velocity V in equations 20 and 21 corresponds to either P- or SV-waves, depending on which attenuation coefficient is desired.

The parameter $\mathcal{H}$ is responsible for the contribution of the attenuation anisotropy. For P-waves at vertical incidence ($\theta = 0^\circ$), $\mathcal{H} = 0$ and $\mathcal{A}_P = 1/(2Q_{33})$; for horizontal direction ($\theta = 90^\circ$), $\mathcal{H} = (Q_{33} - Q_{11})/Q_{11}$ and $\mathcal{A}_P = 1/(2Q_{11})$. Hence, the ratio $(Q_{33} - Q_{11})/Q_{11}$ quantifies the fractional difference between the P-wave attenuation coefficients in the horizontal and the vertical directions and can be used to characterize the P-wave attenuation anisotropy. If $\mathcal{H} = 0$ for all angles, then the P-wave attenuation is isotropic and $\mathcal{A}_P = 1/(2Q_{33})$.

For SV-waves, the value $\mathcal{H} = (Q_{33} - Q_{55})/Q_{55}$ is the same for both the vertical and horizontal directions; the corresponding attenuation coefficient is $\mathcal{A}_{SV} = 1/(2Q_{55})$. Therefore, isotropic SV-wave attenuation implies that $\mathcal{H} = (Q_{33} - Q_{55})/Q_{55}$ for the whole range of angles.

The high accuracy of the approximate solutions for $\mathcal{A}$ is confirmed by the example in Figure 2 generated for a VTI medium with substantial attenuation (the smallest Q-value is 15). The model is elliptical for the velocity anisotropy since $\epsilon = \delta$, but the shape of the attenuation coefficients is strongly nonelliptical. The attenuation coefficients in Figure 2 were computed from equations 19–21 and then substituted into equation B-3 to estimate the real part of the wavenumber and to calculate the slownesses. These approximations practically coincide with the exact solutions for both slowness and attenuation obtained by jointly solving equations B-3 and B-4. (For that reason, the exact curves are not plotted in Figure 2.) This test also demonstrates that the phase velocities are virtually unchanged in the presence of moderate attenuation.

The approximate solution 19 for $\mathcal{A}$ remains accurate even for models with much more significant attenuation and uncommonly large values of the velocity-anisotropy parameters ϵ and δ (Figure 3). In both the vertical ($\theta = 0^\circ$) and horizontal ($\theta = 90^\circ$) directions, the attenuation is independent of ϵ or δ. However, the shape of the attenuation curves at intermediate angles varies with both ϵ and δ, especially when the velocity anisotropy is strong.

THOMSEN-STYLE NOTATION FOR VTI ATTENUATION

The description of seismic signatures in the presence of velocity anisotropy can be simplified substantially by using Thomsen (1986) notation. The advantages of Thomsen parameters in the analysis of seismic velocities and amplitudes for TI media are discussed in detail by Tsvankin (2001).

Here, we extend the principle of Thomsen notation to the directionally dependent attenuation coefficient. The **Q** matrix for models with VTI attenuation contains five independent elements that can be replaced by two reference (isotropic) parameters and three dimensionless coefficients (ϵ_Q, δ_Q, and γ_Q) responsible for the attenuation anisotropy. Since we operate with the attenuation coefficient, which is inversely proportional to the quality factor, the Thomsen-style parameters are convenient to define through quantities $1/Q_{ij}$. To maintain close similarity with Thomsen notation for velocity anisotropy and to make our parameterization suitable for reflection data, we choose the P- and SV-wave attenuation coefficients in the symmetry (vertical) direction as the reference values:

$$\mathcal{A}_{P0} = Q_{33}\left(\sqrt{1+\frac{1}{Q_{33}^2}}-1\right) \approx \frac{1}{2Q_{33}}, \tag{22}$$

$$\mathcal{A}_{S0} = Q_{55}\left(\sqrt{1+\frac{1}{Q_{55}^2}}-1\right) \approx \frac{1}{2Q_{55}}. \tag{23}$$

The coefficient $\mathcal{A}_{S0}$ is also responsible for the SH-wave attenuation in the symmetry (vertical) direction and the SV-wave attenuation in the isotropy plane. Note that the linearization of the square roots in definitions 22 and 23 produces approximate vertical attenuation coefficients accurate to the first order in $1/Q_{ij}$.

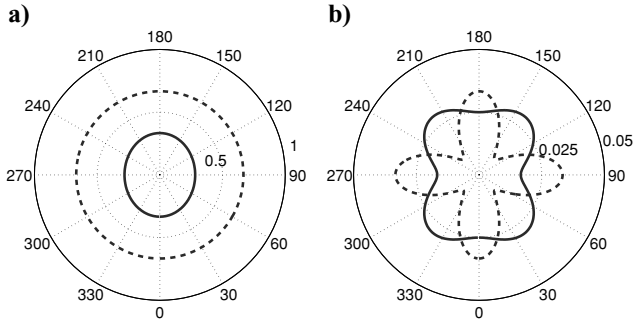

Figure 2. (a) Slownesses and (b) attenuation coefficients $\mathcal{A}$ of P-waves (solid curves) and SV-waves (dashed) as functions of the phase angle with the symmetry axis (numbers on the perimeter). The coefficients $\mathcal{A}$ were computed from approximation 19 and substituted into equation B-3 to obtain the slownesses. The approximations are almost indistinguishable from the exact solutions (not shown). The model parameters are $V_{P0} = 3$ km/s, $V_{S0} = 1.5$ km/s, $\epsilon = \delta = 0.2$, $Q_{11} = 30$, $Q_{33} = 20$, $Q_{13} = 15$, and $Q_{55} = 15$. (The Q-components yield the attenuation-anisotropy parameters $\epsilon_Q = -0.33$ and $\delta_Q = 0.98$.)

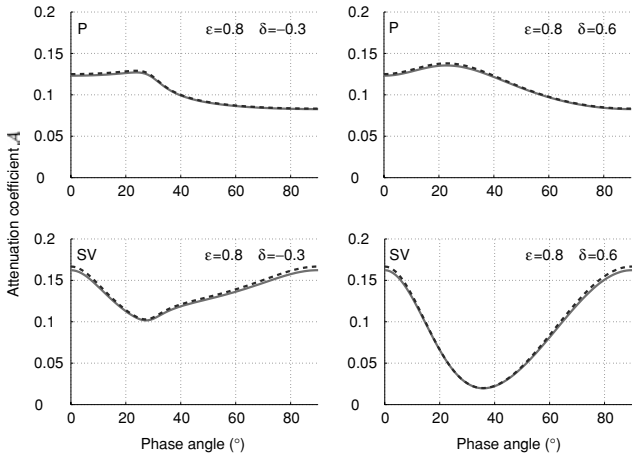

Figure 3. Normalized attenuation coefficients for P-waves (top row) and SV-waves (bottom row) computed for a strongly attenuative, strongly anisotropic medium. The solid curves are the exact solutions from equations B-3 and B-4; the dashed curves represent approximation 19. The two pairs of the parameters ϵ and δ used in the tests are marked on the plots. The other model parameters are $V_{P0} = 3$ km/s, $V_{S0} = 1.5$ km/s, $Q_{11} = 4$, $Q_{33} = 3$, $Q_{13} = 2$, and $Q_{55} = 3$.

SH-wave parameter γ_Q

We define the attenuation-anisotropy parameter γ_Q for SH-waves as the fractional difference between the attenuation coefficients in the horizontal and vertical directions (see equation 18):

$$\gamma_Q \equiv \frac{\dfrac{1}{Q_{66}} - \dfrac{1}{Q_{55}}}{\dfrac{1}{Q_{55}}} = \frac{Q_{55} - Q_{66}}{Q_{66}}. \tag{24}$$

This definition is analogous to that of the Thomsen parameter γ, which is close to the fractional difference between the horizontal and vertical velocities of the SH-wave. The parameter γ_Q controls the magnitude of the SH-wave attenuation anisotropy; for isotropic Q, $\gamma_Q = 0$.

Substituting γ_Q into equation 16 for the parameter α yields

$$\alpha = \frac{(1+2\gamma)\sin^2\theta + \cos^2\theta}{(1+2\gamma)(1+\gamma_Q)\sin^2\theta + \cos^2\theta}. \tag{25}$$

When both γ and γ_Q are small ($|\gamma| \ll 1$, $|\gamma_Q| \ll 1$), α can be linearized in these parameters:

$$\alpha = 1 - \gamma_Q \sin^2\theta. \tag{26}$$

The attenuation coefficient from equation 18 then becomes independent of γ:

$$\mathcal{A}_{SH} = \mathcal{A}_{S0}(1 + \gamma_Q \sin^2\theta), \tag{27}$$

where $\mathcal{A}_{S0}$ is given in equation 23. Equation 27 has the same form as the SH-wave phase velocity linearized in the parameter γ (Thomsen, 1986). Note, however, that the exact phase velocity, unlike the exact attenuation coefficient, is described by a simple function of γ that corresponds to an elliptical slowness surface.

It is clear from equation 27 that γ_Q determines the sign and rate of the variation of $\mathcal{A}_{SH}(\theta)$ away from the vertical (symmetry) direction. When $\gamma_Q > 0$, the factor α decreases with the phase angle θ, which increases the attenuation coefficient (Figure 4a). If the magnitude of the velocity anisotropy is small (i.e., $|\gamma| \ll 1$), approximation 27 gives an accurate estimate of the attenuation coefficient even for relatively large absolute values of γ_Q reaching 0.4 (Figure 4b).

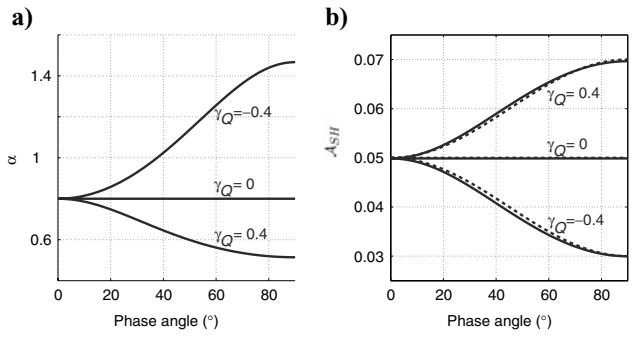

Figure 4. (a) Factor α and (b) SH-wave attenuation coefficient $\mathcal{A}_{SH}$ for a medium with $\gamma = 0.1$, $Q_{55} = 10$, and γ_Q varying from -0.4 to 0.4. The exact $\mathcal{A}_{SH}$ (solid line) is computed from equation 17, and the approximate $\mathcal{A}_{SH}$ (dashed) is computed from equation 27.

P-SV-wave parameters ϵ_Q and δ_Q

The attenuation-anisotropy parameter ϵ_Q can be defined by analogy with the Thomsen parameter ϵ as the fractional difference between the P-wave attenuation coefficients in the horizontal and vertical directions (see also Chichinina et al., 2004):

$$\epsilon_Q \equiv \frac{\dfrac{1}{Q_{11}} - \dfrac{1}{Q_{33}}}{\dfrac{1}{Q_{33}}} = \frac{Q_{33} - Q_{11}}{Q_{11}}. \tag{28}$$

To complete the description of TI attenuation, we need to introduce a parameter similar to Thomsen's δ that involves the Q-factor component Q_{13}. It may seem that the definition of δ (Thomsen, 1986) can be adapted for attenuative media by replacing the stiffnesses c_{ij} with $1/Q_{ij}$:

$$\hat{\delta}_Q \equiv \frac{\left(\frac{1}{Q_{13}} + \frac{1}{Q_{55}}\right)^2 - \left(\frac{1}{Q_{33}} - \frac{1}{Q_{55}}\right)^2}{\frac{2}{Q_{33}}\left(\frac{1}{Q_{33}} - \frac{1}{Q_{55}}\right)}. \tag{29}$$

The parameter $\hat{\delta}_Q$ from equation 29, however, is not physically meaningful. For example, when the attenuation is isotropic and Q_{33}=Q_{55} (Gautam et al., 2003), the anisotropic parameters are supposed to vanish. Instead, $\hat{\delta}_Q$ for isotropic Q goes to infinity.

As discussed by Tsvankin (2001, equation 1.49), δ proved to be extremely useful in describing signatures of reflected P-waves in VTI media because it determines the second derivative of the P-wave phase-velocity function in the vertical (symmetry) direction (the first derivative goes to zero). Therefore, the idea of Thomsen notation can be preserved by defining δ_Q through the second derivative of the P-wave attenuation coefficient $\mathcal{A}_P$ at $\theta = 0$:

$$\delta_Q \equiv \frac{1}{2\mathcal{A}_{P0}} \left.\frac{d^2\mathcal{A}_P}{d\theta^2}\right|_{\theta=0}. \tag{30}$$

In other words, δ_Q controls the curvature of $\mathcal{A}_P(\theta)$ in the vertical direction.

Assuming that both the attenuation and attenuation anisotropy are weak, we find the following explicit expression for δ_Q (Appendix C):

$$\delta_Q \equiv \frac{\frac{Q_{33}-Q_{55}}{Q_{55}} c_{55} \frac{(c_{13}+c_{33})^2}{(c_{33}-c_{55})} + 2\frac{Q_{33}-Q_{13}}{Q_{13}} c_{13}(c_{13}+c_{55})}{c_{33}(c_{33}-c_{55})}. \tag{31}$$

The role of δ_Q in describing the P-wave attenuation anisotropy is similar to that of δ in the P-wave phase-velocity equation (Thomsen, 1986; Tsvankin, 2001). Since the first derivative of $\mathcal{A}_P$ for $\theta = 0$ is zero, δ_Q is responsible for the angular variation of the P-wave attenuation coefficient near the vertical direction.

In the special case of a purely isotropic (i.e., angle-independent) velocity function, δ_Q reduces to a weighted summation of the fractional differences $(Q_{33} - Q_{55})/Q_{55}$ and $(Q_{33} - Q_{13})/Q_{13}$:

$$\delta_Q = \frac{Q_{33} - Q_{55}}{Q_{55}} \frac{4\mu}{\lambda + 2\mu} + \frac{Q_{33} - Q_{13}}{Q_{13}} \frac{2\lambda}{\lambda + 2\mu}, \tag{32}$$

where λ and μ are the Lamé parameters.

Unless attenuation is uncommonly strong, the phase velocities of P- and SV-waves are close to those in the reference nonattenuative medium and do not depend on the attenuation parameters ϵ_Q and δ_Q. Equation 31 for the parameter δ_Q, however, indicates that the attenuation anisotropy is influenced by the velocity anisotropy. If we approximate $c_{13} \approx c_{33}(1+\delta) - 2c_{55}$, which can be done for small $|\delta|$ (Tsvankin, 2001), and denote

$$g \equiv \frac{V_{S0}^2}{V_{P0}^2} = \frac{c_{55}}{c_{33}}, \tag{33}$$

equation 31 for δ_Q can be rewritten as

$$\delta_Q = \frac{Q_{33}-Q_{55}}{Q_{55}} g \frac{(2+\delta-2g)^2}{(1-g)^2} + \frac{Q_{33}-Q_{13}}{Q_{13}} \frac{2(1+\delta-2g)(1+\delta-g)}{(1-g)}. \tag{34}$$

Linearizing equation 34 in g under the assumption $g \ll 1$ leads to the following simplified expression:

$$\delta_Q = 4\frac{Q_{33}-Q_{55}}{Q_{55}} g + 2\frac{Q_{33}-Q_{13}}{Q_{13}}(1+2\delta-2g). \tag{35}$$

Figure 5 shows an example of δ_Q as a function of δ and g. The parameters Q_{33} and Q_{55} are taken from the experimental results of Gautam et al. (2003) for Rim sandstone at a frequency of 25 Hz, while Q_{13} is assigned an arbitrary value. With this choice of the Q-components, the parameter δ_Q is quite sensitive to the squared velocity ratio g and reaches large negative values for hard rocks with $g > 0.35$. While the simplified equation 35 for δ_Q is sufficiently accurate for small magnitudes of both δ and g ($-0.1 < \delta < 0.2$ and $g < 0.2$), it produces a significant error for $g > 0.25$. Note that the absolute value of δ_Q may be large (even greater than unity).

In combination with the Thomsen parameters for the velocity function, the parameters $\mathcal{A}_{P0}$, $\mathcal{A}_{S0}$, ϵ_Q, δ_Q, and γ_Q fully characterize the attenuation of P-, SV-, and SH-waves.

APPROXIMATE ATTENUATION COEFFICIENTS FOR P- AND SV-WAVES

The exact equations for the P- and SV-wave attenuation coefficients are too cumbersome to be represented as explicit functions of the anisotropy-attenuation parameters introduced earlier. It is possible, however, to obtain relatively simple approximations for the coefficient $\mathcal{A}$ by assuming simultaneously (1) weak-attenuation ($1/Q_{ij} \ll 1$); (2) weak-attenuation anisotropy ($|\epsilon_Q| \ll 1, |\delta_Q| \ll 1$); and (3) weak-velocity anisotropy ($|\epsilon| \ll 1, |\delta| \ll 1$). Note that weak attenuation and weak-attenuation anisotropy were already assumed in deriving the P- and SV-wave attenuation coefficients in equations 19–21.

Approximate P-wave attenuation

The approximate P-wave attenuation coefficient can be obtained from equation 19 by expressing the stiffnesses c_{ij} through the Thomsen parameters ϵ and δ and the elements Q_{ij} through the attenuation parameters ϵ_Q and δ_Q. Dropping quadratic terms in $\epsilon, \delta, \epsilon_Q$, and δ_Q yields the following linearized expression:

$$\mathcal{A}_P = \mathcal{A}_{P0}(1 + \delta_Q \sin^2\theta\cos^2\theta + \epsilon_Q \sin^4\theta), \tag{36}$$

where $\mathcal{A}_{P0}$ is defined in equation 22. The angle dependence of the approximate $\mathcal{A}_P$ is governed just by the attenuation-anisotropy parameters ϵ_Q and δ_Q, although δ_Q itself contains a contribution of the velocity anisotropy. The parameter δ_Q is responsible for the attenuation coefficient in near-vertical directions, while ϵ_Q controls $\mathcal{A}_P$ near the horizontal plane. If both ϵ_Q and δ_Q go to zero, the approximate-coefficient $\mathcal{A}_P$ becomes isotropic.

It is noteworthy that equation 36 has the same form as the well-known Thomsen's (1986) weak anisotropy approximation for P-wave phase velocity:

$$V_P = V_{P0}(1 + \delta \sin^2\theta\cos^2\theta + \epsilon \sin^4\theta). \tag{37}$$

To obtain the attenuation coefficient 36 from the phase-velocity equation 37, we need to replace V_{P0} with $\mathcal{A}_{P0}$, ϵ with ϵ_Q, and δ with δ_Q.

Approximate SV-wave attenuation

The SV-wave attenuation coefficient is also obtained by linearizing equation 19:

$$\mathcal{A}_{SV} = \mathcal{A}_{S0}\frac{1 + \left(\frac{2\sigma}{g_Q} + \frac{\epsilon_Q-\delta_Q}{g g_Q}\right)\sin^2\theta\cos^2\theta}{1 + 2\sigma\sin^2\theta\cos^2\theta}, \tag{38}$$

where $\mathcal{A}_{S0}$ and g are defined in equations 23 and 33, respectively; g_Q is given by

$$g_Q \equiv \frac{Q_{33}}{Q_{55}}, \tag{39}$$

and σ is the SV-wave velocity-anisotropy parameter (Tsvankin and Thomsen, 1994; Tsvankin 2001):

$$\sigma \equiv \frac{V_{P0}^2}{V_{S0}^2}(\epsilon-\delta) = \frac{\epsilon-\delta}{g}. \tag{40}$$

If $|\sigma| \ll 1$ and $\left|\frac{2\sigma}{g_Q} + \frac{\epsilon_Q-\delta_Q}{g g_Q}\right| \ll 1$, equation 38 can be simplified further to

$$\mathcal{A}_{SV} = \mathcal{A}_{S0}(1 + \sigma_Q \sin^2\theta\cos^2\theta); \tag{41}$$

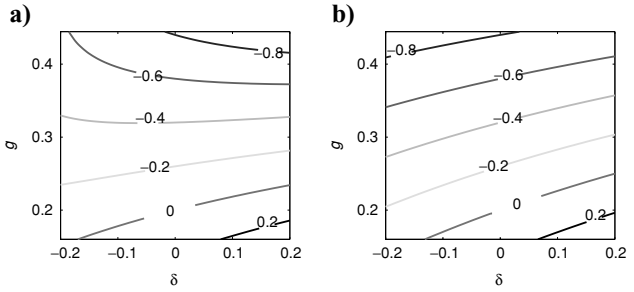

Figure 5. Contour plot of the parameter δ_Q as a function of δ and $g \equiv V_{S0}^2/V_{P0}^2$ computed from (a) equation 31, and (b) equation 35. The other parameters are $Q_{33} = 4$, $Q_{55} = 8$, and $Q_{13} = 3$. The range of g values corresponds to $1.5 < V_{P0}/V_{S0} < 2.5$.

$$\sigma_Q \equiv \frac{1}{g_Q}\left[2(1-g_Q)\sigma + \frac{\epsilon_Q - \delta_Q}{g}\right]. \qquad (42)$$

The parameter σ_Q determines the curvature of the SV-wave attenuation coefficient $\mathcal{A}_{SV}$ in the symmetry direction. The form of equation 41 is identical to that of Thomsen's (1986) approximation for the SV-wave phase velocity in terms of σ. However, σ_Q is a function of both attenuation-anisotropy and velocity-anisotropy parameters. Depending on the sign of σ_Q, the coefficient $\mathcal{A}_{SV}$ has either a maximum or a minimum at $\theta = 45^\circ$.

Note that the assumption $|\sigma| \ll 1$ used in deriving equation 41 may not be valid for many typical TI formations because σ often has a substantial magnitude even when $|\epsilon - \delta|$ is small.

Isotropic attenuation

According to the approximate expression 36, the normalized P-wave attenuation coefficient is isotropic (i.e., independent of angle) if

$$\epsilon_Q = \delta_Q = 0. \qquad (43)$$

Similarly, the coefficient $\mathcal{A}_{SV}$ for SV-waves (equation 41) is isotropic when $\sigma_Q = 0$ or

$$\epsilon_Q - \delta_Q = -2(1-g_Q)(\epsilon - \delta). \qquad (44)$$

The coefficients $\mathcal{A}_P$ and $\mathcal{A}_{SV}$ are both isotropic when $\epsilon_Q = \delta_Q = 0$ and either $g_Q = 1$ or $\epsilon - \delta = 0$ (elliptical anisotropy). The condition $g_Q = 1$, combined with $\epsilon_Q = \delta_Q = 0$, corresponds to the special case of identical Q-components for P-SV waves,

$$Q_{11} = Q_{33} = Q_{13} = Q_{55}, \qquad (45)$$

which yields isotropic normalized attenuation coefficients for P- and SV-waves in VTI media with arbitrary velocity anisotropy. (As discussed earlier, the normalized SH-wave attenuation coefficient is isotropic when $Q_{55} = Q_{66}$, i.e., $\gamma_Q = 0$). The second condition, however, is limited to the approximate attenuation coefficients unless all anisotropy parameters for P- and SV-waves vanish ($\epsilon = \delta = \epsilon_Q = \delta_Q = 0$). Hence, when referring to isotropic attenuation in TI media, one ought to specify the type of plane wave.

The above discussion pertains to the normalized attenuation coefficient $\mathcal{A}$ that characterizes the rate of amplitude decay per wavelength. Alternatively, attenuation can be described by the imaginary wavenumber (i.e., the attenuation coefficient without normalization) denoted here as k^I. Since the wavelength in anisotropic media changes with direction, a model with a purely isotropic coefficient $\mathcal{A}$ generally has an angle-dependent wavenumber k^I. The conditions that make k^I isotropic for all three modes are derived in Appendix D.

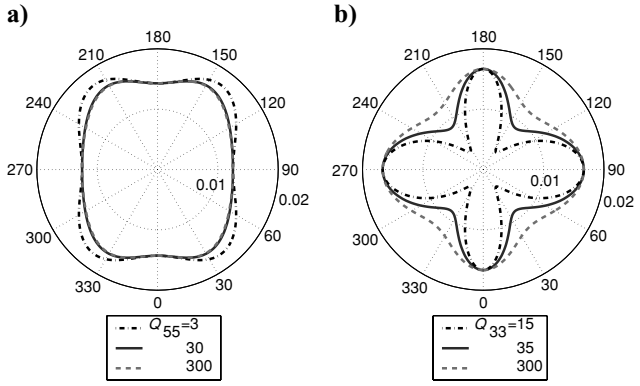

Figure 6. (a) Influence of the parameter $\mathcal{A}_{S0} = 1/(2Q_{55})$ on the normalized P-wave attenuation coefficient; $\mathcal{A}_{P0} = 0.014$ ($Q_{33} = 35$). (b) Influence of the parameter $\mathcal{A}_{P0} = 1/(2Q_{33})$ on the normalized SV-wave attenuation coefficient; $\mathcal{A}_{S0} = 0.017$ ($Q_{55} = 30$). The other model parameters on both plots are $V_{P0} = 2.42$ km/s, $V_{S0} = 1.4$ km/s, $\epsilon = 0.4, \delta = 0.15$, $\epsilon_Q = -0.125$, and $\delta_Q = 0.94$ (δ_Q is computed from equation 31).

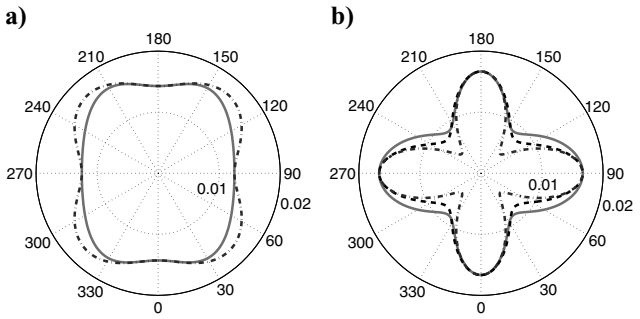

Figure 7. Attenuation coefficients of (a) P-waves and (b) SV-waves as functions of the phase angle. The solid curves are the exact values of $\mathcal{A}$ obtained by jointly solving equations B-3 and B-4; the dashed-dotted curves are the approximate coefficients from equations 36 and 41; the dashed curve on the right plot is the approximate SV-wave coefficient from equation 38. The model parameters are the same as in Figure 6, except for $Q_{33} = 35$ and $Q_{55} = 30$.

Numerical examples

The approximate P-wave attenuation coefficient (equation 36) does not contain the vertical shear-wave attenuation coefficient $\mathcal{A}_{S0}$. Although the linearized approximation becomes inaccurate with increasing magnitude of the anisotropy parameters, $\mathcal{A}_P$ remains independent of $\mathcal{A}_{S0}$ even for models with strong attenuation and pronounced velocity and attenuation anisotropy. As demonstrated in Figure 6a, the variation of the coefficient $\mathcal{A}_P$ with $\mathcal{A}_{S0}$ becomes noticeable only for extremely high attenuation (i.e., uncommonly small values of Q_{55}). Therefore, P-wave attenuation in VTI media is mainly governed by a reduced set of parameters: $\mathcal{A}_{P0}, \epsilon_Q$, and δ_Q. Note that a similar result is valid for the P-wave phase-velocity function that is practically independent of the shear-wave vertical velocity V_{S0} (Tsvankin and Thomsen, 1994; Tsvankin, 2001).

In contrast, SV-wave attenuation is strongly influenced by the vertical P-wave attenuation coefficient $\mathcal{A}_{P0}$ through the parameter σ_Q (Figure 6b). Since σ_Q for this model is negative (for Q_{33} values of 15, 35, and 300, the parameter σ_Q is -4.84, -2.93, and -1.66, respectively), further reduction in Q_{33} results in negative SV-wave attenuation coefficients, which should be considered physically impossible.

The accuracy of the approximate solutions 36, 38, and 41 is illustrated by the numerical tests in Figures 7–11. The P-wave attenuation coefficient in Figure 7 has an extremum

(a maximum) at an angle slightly smaller than 45° because ϵ_Q and δ_Q have opposite signs. If the signs of ϵ_Q and δ_Q are the same, $\mathcal{A}_P$ varies monotonically between the vertical and horizontal directions.

The curve of $\mathcal{A}_{SV}$ has a concave shape because σ_Q in equation 41 is negative and large by absolute value. Approximations 38 and 41 predict a minimum of the SV-wave attenuation coefficient at $\theta = 45°$. The extrema of the exact coefficients $\mathcal{A}$ in Figure 7 (solid lines) for both P- and SV-waves, however, are somewhat shifted toward the vertical axis with respect to their approximate positions.

The linearized expressions for the attenuation coefficients give satisfactory results for near-vertical propagation directions with angles θ up to about 30°. The error becomes noticeable for intermediate angles $30° < \theta < 75°$ and then decreases again near the horizontal plane. Note that the velocity (see Figure 8) and attenuation anisotropy for the model from Figure 7 cannot be considered weak, and the values of $\sigma = 0.75$ and $\sigma_Q = -2.93$ are particularly large. Since equation 38 does not assume that σ and $[(2\sigma/g_Q) + (\epsilon_Q - \delta_Q)/(gg_Q)] = (2\sigma + \sigma_Q)$ are small by absolute value, it provides a better approximation for the SV-wave attenuation coefficient than does equation 41.

For models with smaller magnitudes of the anisotropy parameters (Figure 9), equations 36 and 41 become sufficiently accurate for the attenuation coefficients in the full range of phase angles. Our tests show that the error of the approximate solutions 36, 38, and 41 is controlled primarily by the strength of the velocity anisotropy, even if the magnitude of the attenuation anisotropy is much higher.

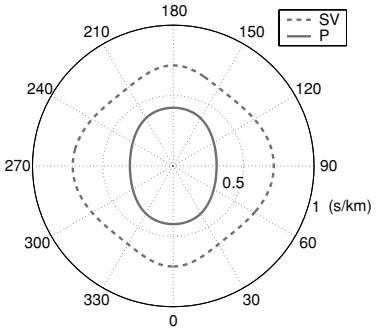

Figure 8. Slownesses (s/km) of P-waves (solid curves) and SV-waves (dashed curves) for the model from Figure 7.

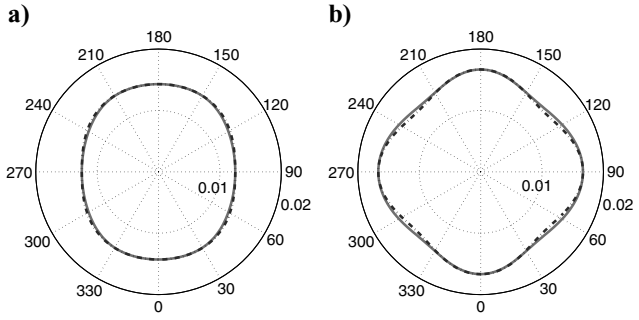

Figure 9. Attenuation coefficients of (a) P-waves and (b) SV-waves for $V_{P0} = 2.42$ km/s, $V_{S0} = 1.4$ km/s, $\epsilon = 0.125$, $\delta = -0.05$, $Q_{33} = 35$, $Q_{55} = 30$, $\epsilon_Q = -0.125$, and $\delta_Q = 0.05$. The solid curves are the exact values of $\mathcal{A}$ obtained by jointly solving equations B-3 and B-4; the dashed-dotted curves are the approximate coefficients from equations 36 and 41.

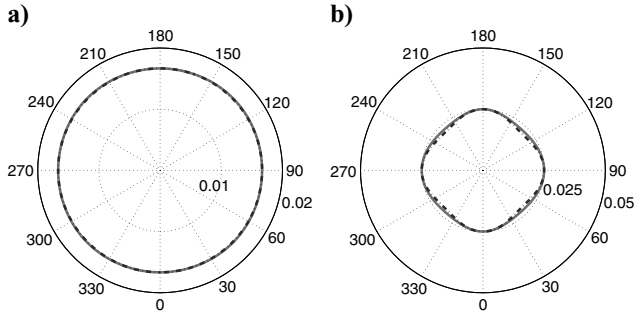

Figure 10. Attenuation coefficients of (a) P-waves and (b) SV-waves for $\epsilon = 0.4$, $\delta = 0.15$, and $\epsilon_Q = \delta_Q = 0$. The solid curves are the exact values of $\mathcal{A}$ obtained by jointly solving equations B-3 and B-4; the dashed-dotted curves are the approximate coefficients from equations 36 and 41. The other model parameters are the same as those in Figure 9.

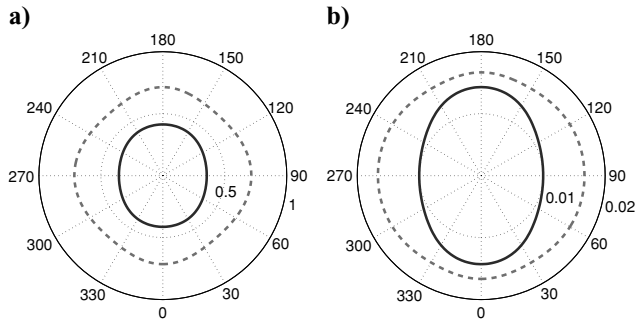

Figure 11. Exact (a) slownesses and (b) attenuation coefficients $\mathcal{A}$ of P-waves (solid curves) and SV-waves (dashed) for a medium with the isotropic condition for SV-wave attenuation ($\sigma_Q = 0$). The model parameters are $V_{P0} = 2.42$ km/s, $V_{S0} = 1.4$ km/s, $\epsilon = 0.18$, $\delta = 0.05$, $Q_{33} = 35$, $Q_{55} = 30$, $\epsilon_Q = -0.30$, and $\delta_Q = -0.40$ (ϵ_Q and δ_Q satisfy equation 44).

Figure 10 displays the attenuation coefficients for a medium with $\epsilon_Q = \delta_Q = 0$. The approximate P-wave attenuation computed from equation 36 in this case is isotropic. However, the exact coefficient $\mathcal{A}_P$ deviates slightly from a circle, which indicates the nonnegligible influence of quadratic and higher-order terms in the parameters ϵ_Q and δ_Q. Also, the attenuation coefficient of SV-waves varies with angle because of the contribution of the velocity anisotropy (i.e., of the term involving σ) in equation 41. If the condition $\epsilon_Q = \delta_Q = 0$ is supplemented by $g_Q = 1$, all Q_{ij} become identical, and both P- and SV-wave attenuation coefficients are independent of direction no matter how strong the velocity anisotropy is.

If ϵ_Q and δ_Q satisfy condition 44 that results in $\sigma_Q = 0$ (Figure 11), the exact SV-wave attenuation coefficient is almost constant, although some deviations from a circle are visible. The curve of the P-wave coefficient $\mathcal{A}_P$ closely resembles an ellipse, but elliptical attenuation anisotropy for P-waves requires that $\epsilon_Q = \delta_Q$.

DISCUSSION AND CONCLUSIONS

The main goal of this paper was to build a practical, analytic framework for describing attenuation-related amplitude distortions in TI media. Although the symmetry axis was taken to be vertical, all results can be applied for TI media with an arbitrary axis orientation. Under the assumption of weak attenuation, we restricted the discussion to homogeneous-wave-propagation by taking the real and the imaginary parts of the wave vector to be parallel to one another. For layered attenuative models, however, the assumption of homogeneity may cause errors in the estimation of attenuation coefficients.

When attenuation is directionally dependent, the quality factor Q becomes a matrix with each component Q_{ij} defined as the ratio of the real and the imaginary parts of the corresponding stiffness coefficient. The **Q**-matrix has a purely isotropic structure if it includes just two independent elements responsible for the attenuation coefficients of P- and S-waves along the symmetry axis. For the special case of identical Q_{ij} components, plane-wave attenuation is independent of propagation direction, even for arbitrary velocity anisotropy.

It seems plausible that the attenuation anisotropy, defined by the structure of the **Q** matrix, has the same or higher symmetry as the velocity anisotropy. Here, we treated TI velocity models with either TI or isotropic attenuation and assumed that the symmetry axes for the velocity and attenuation anisotropy are aligned. Analysis of the Christoffel equation for this model shows that the perturbation of the phase-velocity function caused by the attenuation is of the second order and can be ignored.

To facilitate the description of TI attenuation, we introduced Thomsen-style parameters responsible for directionally dependent attenuation coefficients of P-, SV-, and SH-waves. The reference isotropic values are the P- and S-wave attenuation coefficients in the vertical (symmetry) direction ($\mathcal{A}_{P0}$ and $\mathcal{A}_{S0}$). Following the idea of Thomsen's notation for velocity anisotropy, we supplemented the reference quantities with three dimensionless anisotropic parameters denoted by ϵ_Q, δ_Q, and γ_Q.

The parameter ϵ_Q is equal to the fractional difference between the P-wave horizontal and vertical attenuation coefficients, and γ_Q denotes the same quantity for SH-waves. Similar to the Thomsen parameter δ for velocity anisotropy, δ_Q is designed to describe near-vertical variations in P-wave attenuation. We defined δ_Q as the normalized second derivative of the P-wave attenuation coefficient at vertical incidence. In contrast to ϵ_Q and γ_Q, the parameter δ_Q depends on δ and therefore reflects the coupling between the attenuation and velocity anisotropy. If the frequency dependence of the Q-factor and phase velocity for seismic bandwidth cannot be ignored, the attenuation-anisotropy parameters also become functions of frequency. However, this does not formally change our definitions of ϵ_Q, δ_Q, and γ_Q.

While the attenuation coefficient of SH-waves can be expressed straightforwardly through the parameter γ_Q, exact equations for the attenuation anisotropy of P- and SV-waves are much more involved. The Thomsen-style parameters, however, can be used to obtain the linearized attenuation coefficients under the assumptions of weak attenuation and of weak velocity and attenuation anisotropy. The approximate P-wave attenuation coefficient has the same form as the linearized phase-velocity function, with the vertical velocity V_{P0} replaced by $\mathcal{A}_{P0}$, ϵ by ϵ_Q, and δ by δ_Q. Although the approximate solution for the attenuation coefficient for SV-waves involves contributions of both attenuation and velocity parameters, it has the same-angle dependence as its phase-velocity counterpart.

Numerical examples demonstrate that the approximate solutions adequately reproduce the character of attenuation anisotropy and are sufficiently accurate for moderately anisotropic (in terms of both velocity and attenuation) TI models. The exact P-wave attenuation coefficient in strongly anisotropic media remains a function of just three parameters: $\mathcal{A}_{P0}$, ϵ_Q, and δ_Q. Computation of the exact attenuation coefficients also confirms that the isotropic **Q** matrix in TI media does not necessarily yield isotropic (i.e., independent of direction) attenuation of P- and SV-waves because of the influence of the velocity anisotropy.

ACKNOWLEDGMENTS

We are grateful to Michael Batzle and Maarten de Hoop (Colorado School of Mines), Ivan Pšenčík (Czech Academy of Sciences), Tatiana Chichinina (Instituto Mexicano del Petroleo, Mexico City), and members of the A(nisotropy)-Team of the Center for Wave Phenomena (CWP) at Colorado School of Mines for useful discussions. We also thank Michael Slawinski, Edward Krebes, José M. Carcione, and an anonymous reviewer for constructive comments. The support for this work was provided by the Consortium Project on Seismic Inverse Methods for Complex Structures at CWP and by the Chemical Sciences, Geosciences and Biosciences Division, Office of Basic Energy Sciences, U. S. Department of Energy.

APPENDIX A

PLANE SH-WAVES IN ATTENUATIVE VTI MEDIA

The Christoffel equation for a plane SH-wave propagating in an attenuative VTI medium yields

$$\tilde{c}_{66}\tilde{k}_1^2 + \tilde{c}_{55}\tilde{k}_3^2 - \rho\omega^2 = 0, \tag{A-1}$$

where $\tilde{c}_{ij} = c_{ij} + ic_{ij}^I$ are the complex stiffness coefficients. The complex wavenumber is represented as $\tilde{k}_i = k_i - ik_i^I$, where $k^I = \sqrt{k_1^{I2} + k_2^{I2} + k_3^{I2}}$ is the attenuation coefficient.

VTI Q matrix: Inhomogeneous wave-propagation

First, we consider the general case of inhomogeneous-wave-propagation and allow the vectors **k** and $\mathbf{k}^I$ to make different angles (θ and θ^I, respectively) with the vertical symmetry axis. If the **Q** matrix has VTI symmetry, equation A-1 becomes

$$c_{66}\left(1 + \frac{i}{Q_{66}}\right)(k\sin\theta - ik^I\sin\theta^I)^2 + c_{55}\left(1 + \frac{i}{Q_{55}}\right)(k\cos\theta - ik^I\cos\theta^I)^2 - \rho\omega^2 = 0. \tag{A-2}$$

Equation A-2 can be separated into the real part,

$$c_{66}\left[k^2\sin^2\theta - (k^I)^2\sin^2\theta^I + \frac{1}{Q_{66}}2kk^I\sin\theta\sin\theta^I\right]$$

$$+c_{55}\left[k^2\cos^2\theta-(k^I)^2\cos^2\theta^I+\frac{1}{Q_{55}}2kk^I\cos\theta\cos\theta^I\right]-\rho\omega^2=0, \tag{A-3}$$

and the imaginary part,

$$c_{66}\left[\frac{1}{Q_{66}}(k^2\sin^2\theta-(k^I)^2\sin^2\theta^I)-2kk^I\sin\theta\sin\theta^I\right]+c_{55}\left[\frac{1}{Q_{55}}\left(k^2\cos^2\theta-(k^I)^2\cos^2\theta^I\right)-2kk^I\cos\theta\cos\theta^I\right]=0. \tag{A-4}$$

By introducing the SH-wave velocity-anisotropy parameter $\gamma\equiv(c_{66}-c_{55})/(2c_{55})$ (Thomsen, 1986), equation A-4 can be rewritten as

$$k^2\left[(1+2\gamma)\frac{Q_{55}}{Q_{66}}\sin^2\theta+\cos^2\theta\right]-(k^I)^2\left[(1+2\gamma)\frac{Q_{55}}{Q_{66}}\sin^2\theta^I+\cos^2\theta^I\right]-2kk^IQ_{55}[(1+2\gamma)\sin\theta\sin\theta^I+\cos\theta\cos\theta^I]=0. \tag{A-5}$$

The only physically meaningful solution of equation A-5 is given by

$$\frac{k^I}{k}=\left\{\sqrt{1+\frac{\left[(1+2\gamma)\frac{Q_{55}}{Q_{66}}\sin^2\theta+\cos^2\theta\right]\left[(1+2\gamma)\frac{Q_{55}}{Q_{66}}\sin^2\theta^I+\cos^2\theta^I\right]}{Q_{55}^2[\cos(\theta^I-\theta)+2\gamma\sin\theta\sin\theta^I]^2}}-1\right\}\times\frac{Q_{55}[\cos(\theta^I-\theta)+2\gamma\sin\theta\sin\theta^I]}{\left[(1+2\gamma)\frac{Q_{55}}{Q_{66}}\sin^2\theta^I+\cos^2\theta^I\right]}. \tag{A-6}$$

For weakly attenuative media with $Q_{55}\to\infty$, the term $Q_{55}|\cos(\theta^I-\theta)|$ is much greater than unity if the inhomogeneity angle $\theta^I-\theta\neq\pm90^\circ$. Although it is possible for the conditions $Q_{55}\to\infty$ and $\theta^I-\theta=\pm90^\circ$ to be satisfied simultaneously, models of this kind are not typical (Krebes and Slawinski, 1991). Then the square root in equation A-6 can be expanded in the small parameter $1/[Q_{55}^2\cos^2(\theta^I-\theta)]$. Retaining only the linear term in this parameter, we obtain

$$\frac{k^I}{k}=\frac{1}{2Q_{55}}\frac{(1+2\gamma)\frac{Q_{55}}{Q_{66}}\sin^2\theta+\cos^2\theta}{\cos(\theta^I-\theta)+2\gamma\sin\theta\sin\theta^I}. \tag{A-7}$$

If attenuation is weak ($1/Q_{55}\ll1$ and $1/Q_{66}\ll1$), the inhomogeneity angle $\theta^I-\theta$ that appears in problems involving point sources in homogeneous media is small so that $|\sin(\theta^I-\theta)|\ll1$ (Ben-Menahem and Singh, 1981). In this case, the contribution of the inhomogeneity angle in equation A-7 is of the second order. Indeed, $\cos(\theta^I-\theta)\approx1-(\theta^I-\theta)^2/2$, while $\sin\theta^I$ can be represented as

$$\sin\theta^I=\sin\theta\cos(\theta^I-\theta)+\cos\theta\sin(\theta^I-\theta). \tag{A-8}$$

Note that in equation A-7, $\sin\theta^I$ is multiplied with the Thomsen parameter γ. Therefore, if the velocity anisotropy is weak ($|\gamma|\ll1$), all terms involving the inhomogeneity angle in the denominator of equation A-7 are quadratic or higher order in the small parameters. When we further assume that the attenuation anisotropy is weak ($|(Q_{55}-Q_{66})/Q_{66}|\ll1$), equation A-7 can be simplified by dropping all quadratic terms in the parameters $\sin(\theta^I-\theta)$, γ, and $(Q_{55}-Q_{66})/Q_{66}$:

$$\frac{k^I}{k}=\frac{1}{2Q_{55}}\left(1+\frac{Q_{55}-Q_{66}}{Q_{66}}\sin^2\theta\right). \tag{A-9}$$

Analysis of the phase-velocity function (equation A-3) in the limit of small attenuation and of weak attenuation and velocity anisotropy (not shown here) leads to a similar result: As long as the inhomogeneity angle is small, it contributes only to second-order terms.

VTI Q matrix: Homogeneous wave-propagation

For homogeneous wave-propagation ($\theta^I=\theta$), equation A-5 takes a much simpler form:

$$k^2-(k^I)^2-2Q_{55}\alpha kk^I=0, \tag{A-10}$$

where

$$\alpha\equiv\frac{(1+2\gamma)\sin^2\theta+\cos^2\theta}{(1+2\gamma)\frac{Q_{55}}{Q_{66}}\sin^2\theta+\cos^2\theta}. \tag{A-11}$$

The physically meaningful solution is

$$\frac{k^I}{k}=\sqrt{1+(Q_{55}\alpha)^2}-Q_{55}\alpha. \tag{A-12}$$

The real part of the Christoffel equation (equation A-3) then reduces to

$$(c_{66}\sin^2\theta+c_{55}\cos^2\theta)\left[k^2-(k^I)^2+\frac{2kk^I}{Q_{55}\alpha}\right]-\rho\omega^2=0. \tag{A-13}$$

The phase velocity of SH-waves is found as

$$V_{SH}=\frac{\omega}{k}=\xi_QV_{SH}^{\text{elast}}, \tag{A-14}$$

where V_{SH}^{elast} is the phase velocity in purely elastic VTI media,

$$V_{SH}^{\text{elast}}=\sqrt{\frac{c_{66}\sin^2\theta+c_{55}\cos^2\theta}{\rho}}, \tag{A-15}$$

and ξ_Q is the factor responsible for the influence of the anisotropic attenuation:

$$\xi_Q\equiv\sqrt{\frac{2\left(\sqrt{1+(Q_{55}\alpha)^2}-Q_{55}\alpha\right)(1+(Q_{55}\alpha)^2)}{Q_{55}\alpha}}. \tag{A-16}$$

For weak attenuation, $\xi_Q\approx1+\frac{1}{2(Q_{55}\alpha)^2}$.

Isotropic Q matrix

Isotropic Q for the SH-wave propagation implies $Q_{55}=Q_{66}$. Taking into account that $\alpha=1$, the imaginary part of equation A-1 reduces to

$$k^2-(k^I)^2-2Qkk^I=0. \tag{A-17}$$

Hence, for isotropic Q we find

$$k^I=k(\sqrt{1+Q^2}-Q), \tag{A-18}$$

and

$$\xi_Q = \sqrt{\frac{2(\sqrt{1+Q^2}-Q)(1+Q^2)}{Q}}. \quad \text{(A-19)}$$

APPENDIX B

PLANE P- AND SV-WAVES IN ATTENUATIVE VTI MEDIA

For P- and SV-waves, the Christoffel equation 6 can be written as

$$\left(\tilde{c}_{11}\tilde{k}_1^2 + \tilde{c}_{55}\tilde{k}_3^2 - \rho\omega^2\right)\left(\tilde{c}_{55}\tilde{k}_1^2 + \tilde{c}_{33}\tilde{k}_3^2 - \rho\omega^2\right) - \left[(\tilde{c}_{13}+\tilde{c}_{55})\tilde{k}_1\tilde{k}_3\right]^2 = 0. \quad \text{(B-1)}$$

Analysis of the attenuation coefficients and phase velocities of P- and SV-waves in the limit of small attenuation and weak attenuation and velocity anisotropy shows that the inhomogeneity angle contributes only to second-order terms (see the analysis for SH-waves in Appendix A). Hence, this discussion is limited to homogeneous P- and SV-wave propagation.

VTI Q matrix

When the **Q** matrix has VTI symmetry, equation B-1 yields

$$\left\{\left[\left(c_{11}+ic_{11}^I\right)\sin^2\theta + \left(c_{55}+ic_{55}^I\right)\cos^2\theta\right](k-ik^I)^2 - \rho\omega^2\right\} \times \left\{\left[\left(c_{55}+ic_{55}^I\right)\sin^2\theta + \left(c_{33}+ic_{33}^I\right)\cos^2\theta\right](k-ik^I)^2 - \rho\omega^2\right\} - \left\{\left[(c_{13}+c_{55}) + i\left(c_{13}^I + c_{55}^I\right)\right]\sin\theta\cos\theta k k^I\right\}^2 = 0. \quad \text{(B-2)}$$

The real and the imaginary parts are given, respectively, by

$$\begin{aligned}&[(c_{11}\sin^2\theta + c_{55}\cos^2\theta)\mathcal{K}_1^a - \rho\omega^2] \\ &\times [(c_{55}\sin^2\theta + c_{33}\cos^2\theta)\mathcal{K}_1^b - \rho\omega^2] \\ &- (c_{11}\sin^2\theta + c_{55}\cos^2\theta)(c_{55}\sin^2\theta + c_{33}\cos^2\theta)\mathcal{K}_2^a\mathcal{K}_2^b \\ &- (c_{13}+c_{55})^2\sin^2\theta\cos^2\theta\left[\left(\mathcal{K}_1^c\right)^2 - \left(\mathcal{K}_2^c\right)^2\right] = 0 \end{aligned} \quad \text{(B-3)}$$

and

$$\begin{aligned}&(c_{11}\sin^2\theta + c_{55}\cos^2\theta)\mathcal{K}_2^a \\ &\quad\times\left[(c_{55}\sin^2\theta + c_{33}\cos^2\theta)\mathcal{K}_1^b - \rho\omega^2\right] \\ &\quad+(c_{55}\sin^2\theta + c_{33}\cos^2\theta)\mathcal{K}_2^b \\ &\quad\times\left[(c_{11}\sin^2\theta + c_{55}\cos^2\theta)\mathcal{K}_1^a - \rho\omega^2\right] \\ &\quad-(c_{13}+c_{55})^2\sin^2\theta\cos^2\theta 2\mathcal{K}_1^c\mathcal{K}_2^c = 0, \end{aligned} \quad \text{(B-4)}$$

where

$$\begin{aligned}\mathcal{K}_1^a &= \mathcal{K}_1 + \frac{\Delta^a}{Q_{33}}2kk^I, \quad \mathcal{K}_2^a = \mathcal{K}_2 - \frac{\Delta^a}{Q_{33}}[k^2-(k^I)^2], \\ \mathcal{K}_1^b &= \mathcal{K}_1 + \frac{\Delta^b}{Q_{33}}2kk^I, \quad \mathcal{K}_2^b = \mathcal{K}_2 - \frac{\Delta^b}{Q_{33}}[k^2-(k^I)^2], \\ \mathcal{K}_1^c &= \mathcal{K}_1 + \frac{\Delta^c}{Q_{33}}2kk^I, \quad \mathcal{K}_2^c = \mathcal{K}_2 - \frac{\Delta^c}{Q_{33}}[k^2-(k^I)^2],\end{aligned} \quad \text{(B-5)}$$

$$\mathcal{K}_1 = k^2 - (k^I)^2 + \frac{2kk^I}{Q_{33}}, \quad \text{(B-6)}$$

$$\mathcal{K}_2 = \frac{1}{Q_{33}}[k^2-(k^I)^2] - 2kk^I, \quad \text{(B-7)}$$

and

$$\begin{aligned}\Delta^a &= \frac{c_{11}\sin^2\theta}{c_{11}\sin^2\theta + c_{55}\cos^2\theta}\frac{Q_{33}-Q_{11}}{Q_{11}} + \frac{c_{55}\cos^2\theta}{c_{11}\sin^2\theta + c_{55}\cos^2\theta}\frac{Q_{33}-Q_{55}}{Q_{55}}, \\ \Delta^b &= \frac{c_{55}\sin^2\theta}{c_{55}\sin^2\theta + c_{33}\cos^2\theta}\frac{Q_{33}-Q_{55}}{Q_{55}}, \\ \Delta^c &= \frac{c_{13}}{c_{13}+c_{55}}\frac{Q_{33}-Q_{13}}{Q_{13}} + \frac{c_{55}}{c_{13}+c_{55}}\frac{Q_{33}-Q_{55}}{Q_{55}}.\end{aligned} \quad \text{(B-8)}$$

Using equation B-4, we find

$$\mathcal{K}_2 = -\frac{A\Delta^a + B\Delta^b - C\Delta^c}{A+B-C}\frac{[k^2-(k^I)^2]}{Q_{33}}, \quad \text{(B-9)}$$

where

$$\begin{aligned}A &= (c_{11}\sin^2\theta + c_{55}\cos^2\theta) \\ &\quad\times\left[(c_{55}\sin^2\theta + c_{33}\cos^2\theta)\mathcal{K}_1^b - \rho\omega^2\right], \\ B &= (c_{55}\sin^2\theta + c_{33}\cos^2\theta) \\ &\quad\times\left[(c_{11}\sin^2\theta + c_{55}\cos^2\theta)\mathcal{K}_1^a - \rho\omega^2\right], \\ C &= 2(c_{13}+c_{55})^2\sin^2\theta\cos^2\theta\mathcal{K}_1^c.\end{aligned} \quad \text{(B-10)}$$

Equations B-7 and B-9 can be combined to solve for the normalized attenuation coefficient $\mathcal{A} \equiv k^I/k$. As shown in Appendix C, equation B-9 can be simplified by assuming weak attenuation and weak-attenuation anisotropy.

Special case: $Q_{ij} \equiv Q$

For the special case of identical Q-components, $c_{11}/c_{11}^I = c_{33}/c_{33}^I = c_{13}/c_{13}^I = c_{55}/c_{55}^I = Q$, equation B-1 becomes

$$\begin{aligned}&[(c_{11}\sin^2\theta + c_{55}\cos^2\theta)\mathcal{K}_1 - \rho\omega^2 \\ &\quad+i(c_{11}\sin^2\theta + c_{55}\cos^2\theta)\mathcal{K}_2] \\ &\quad\times[(c_{55}\sin^2\theta + c_{33}\cos^2\theta)\mathcal{K}_1 - \rho\omega^2 \\ &\quad+i(c_{55}\sin^2\theta + c_{33}\cos^2\theta)\mathcal{K}_2] \\ &\quad-[(c_{13}+c_{55})\sin\theta\cos\theta(\mathcal{K}_1 + i\mathcal{K}_2)]^2 = 0, \end{aligned} \quad \text{(B-11)}$$

where $\mathcal{K}_1$ and $\mathcal{K}_2$ are defined in equations B-6 and B-7 with Q_{33} replaced by Q.

The only physically meaningful solution of the imaginary part of equation B-11 is $\mathcal{K}_2 = 0$, which then yields the same isotropic expression for k^I as that in equation A-18.

Solving the real part of equation B-11, we obtain the phase velocities in the form

$$V_{\{P,SV\}} = \xi_Q V_{\{P,SV\}}^{\text{elast}}, \quad \text{(B-12)}$$

where ξ_Q is given in equation A-19 and $V_{\{P,SV\}}^{\text{elast}}$ is the P- or SV-wave phase velocity in the reference purely elastic VTI medium:

$$V_{\{P,SV\}}^{\text{elast}} = \frac{1}{\sqrt{2\rho}}\left\{(c_{11}+c_{55})\sin^2\theta + (c_{33}+c_{55})\cos^2\theta \pm \sqrt{[(c_{11}-c_{55})\sin^2\theta - (c_{33}-c_{55})\cos^2\theta]^2 + 4(c_{13}+c_{55})^2\sin^2\theta\cos^2\theta}\right\}^{1/2}. \quad \text{(B-13)}$$

APPENDIX C

APPROXIMATE SOLUTIONS FOR WEAK ATTENUATION AND WEAK ATTENUATION ANISOTROPY

Here we simplify the attenuation coefficient derived in Appendix B for homogeneous wave-propagation under the assumption of weak attenuation and weak attenuation anisotropy.

Attenuation coefficients for P- and SV-waves

For weak attenuation ($k^I \ll k$), the term $(k^I)^2$ in the difference $k^2 - (k^I)^2$ can be dropped. If the attenuation anisotropy is weak, then the fractional difference between the P-wave attenuation coefficients in the horizontal and vertical directions is small and $\left|(Q_{33} - Q_{11})/Q_{11}\right| \ll 1$. When Q_{33} and Q_{55} are comparable (a common case), the assumption of weak-attenuation anisotropy implies that Q_{13} is comparable to (i.e., of the same order as) Q_{33} and Q_{55} (it follows from the definition of the parameter δ_Q). Hence, the magnitude of the terms Δ^a, Δ^b, and Δ^c in equation B-8 is not much larger than unity. Then the terms $(\Delta^a/Q_{33})2kk^I$, $(\Delta^b/Q_{33})2kk^I$, and $(\Delta^c/Q_{33})2kk^I$ in equations B-5 are of the second order compared to k^2, and $\mathcal{K}_1^a \approx \mathcal{K}_1^b \approx \mathcal{K}_1^c \approx \mathcal{K}_1$. It follows from equation B-6 that for weak attenuation $\mathcal{K}_1 \approx k^2$, which allows us to represent equations B-10 as

$$\begin{aligned} A &= (c_{11}\sin^2\theta + c_{55}\cos^2\theta)[(c_{55}\sin^2\theta \\ &\quad + c_{33}\cos^2\theta)k^2 - \rho\omega^2], \\ B &= (c_{55}\sin^2\theta + c_{33}\cos^2\theta)[(c_{11}\sin^2\theta \\ &\quad + c_{55}\cos^2\theta)k^2 - \rho\omega^2], \\ C &= 2(c_{13} + c_{55})^2\sin^2\theta\cos^2\theta k^2. \end{aligned} \tag{C-1}$$

Combining equations B-7 and B-9 in the limit of weak attenuation, we find

$$k^2 - 2Q_{33}kk^I = -\frac{A\Delta^a + B\Delta^b - C\Delta^c}{A + B - C}k^2. \tag{C-2}$$

Substituting equations C-1 into equation C-2 yields

$$\mathcal{A} = \frac{1}{2Q_{33}}(1 + \mathcal{H}), \tag{C-3}$$

where

$$\mathcal{H} \equiv \frac{A\Delta^a + B\Delta^b - C\Delta^c}{A + B - C}. \tag{C-4}$$

Parameter δ_Q

The attenuation-anisotropy parameter δ_Q is defined through the second derivative of the normalized P-wave attenuation coefficient $\mathcal{A}_P$ with respect to the phase-angle θ at vertical incidence:

$$\left.\frac{d^2\mathcal{A}_P}{d\theta^2}\right|_{\theta=0} = 2\mathcal{A}_{P0}\,\delta_Q. \tag{C-5}$$

Substitution of $\mathcal{A}_P$ from equation C-3 leads to the following expression for δ_Q under the assumption of weak attenuation and weak attenuation anisotropy:

$$\delta_Q = \frac{1}{2}\left.\frac{d^2\mathcal{H}}{d\theta^2}\right|_{\theta=0}. \tag{C-6}$$

By evaluating $d^2\mathcal{H}/d\theta^2|_{\theta=0}$ and taking into account that for P-waves $\mathcal{H}|_{\theta=0} = 0$ and $\partial\mathcal{H}/\partial\theta|_{\theta=0} = 0$, we obtain

$$\delta_Q = \frac{\frac{Q_{33}-Q_{55}}{Q_{55}}c_{55}\frac{(c_{13}+c_{33})^2}{(c_{33}-c_{55})} + 2\frac{Q_{33}-Q_{13}}{Q_{13}}c_{13}(c_{13}+c_{55})}{c_{33}(c_{33}-c_{55})}. \tag{C-7}$$

APPENDIX D

ISOTROPIC CONDITIONS FOR THE ATTENUATION COEFFICIENT k^I

In the main text, we discuss the conditions needed to make the normalized attenuation coefficient $\mathcal{A}$ isotropic (independent of angle). For completeness, here we introduce the isotropic conditions for the imaginary wavenumber (attenuation coefficient) k^I. The attenuation and velocity anisotropy, as well as the attenuation itself, are assumed to be weak.

SH-wave

We find the approximate SH-wave attenuation coefficient by substituting the SH-wave phase-velocity V_{SH} as a function of the phase-angle θ into equation 27:

$$\begin{aligned} k^I_{SH} &= \frac{\omega}{V_{SH}(\theta)}\mathcal{A}_{SH} \\ &= \frac{\omega}{2Q_{55}V_{S0}}\frac{1 + \gamma_Q\sin^2\theta}{\sqrt{1 + 2\gamma\sin^2\theta}}, \end{aligned} \tag{D-1}$$

where ω is the angular frequency and V_{S0} is the shear-wave velocity along the symmetry axis. If $|\gamma| \ll 1$, equation D-1 simplifies to

$$k^I_{SH} = \frac{\omega}{2Q_{55}V_{S0}}[1 + (\gamma_Q - \gamma)\sin^2\theta]. \tag{D-2}$$

The coefficient k^I_{SH} is independent of angle only if

$$\gamma = \gamma_Q. \tag{D-3}$$

P–SV-waves

Using the linearized phase-velocity functions (Thomsen, 1986), the P- and SV-wave attenuation coefficients can be obtained from equations 36 and 41 as

$$\begin{aligned} k^I_P &= \frac{\omega}{V_P(\theta)}\mathcal{A}_P \\ &= \frac{\omega}{2Q_{33}V_{P0}}\frac{1 + \delta_Q\sin^2\theta\cos^2\theta + \epsilon_Q\sin^4\theta}{1 + \delta\sin^2\theta\cos^2\theta + \epsilon\sin^4\theta}, \end{aligned} \tag{D-4}$$

$$k^I_{SV} = \frac{\omega}{V_{SV}(\theta)}\mathcal{A}_{SV} = \frac{\omega}{2Q_{55}V_{S0}}\frac{1 + \sigma_Q\sin^2\theta}{1 + \sigma\sin^2\theta}. \tag{D-5}$$

The coefficient k^I_P becomes isotropic if

$$\epsilon = \epsilon_Q \quad \text{and} \quad \delta = \delta_Q. \tag{D-6}$$

Isotropic k^I_{SV} requires that

$$\sigma = \sigma_Q. \tag{D-7}$$

Both k^I_P and k^I_{SV} are independent of angle if the anisotropic parameters satisfy equation D-6 and, as follows from equation 42,

$$g_Q \equiv \frac{Q_{33}}{Q_{55}} = 1. \tag{D-8}$$

Therefore, unlike the normalized attenuation coefficient, the imaginary wavenumber k^I does not necessarily become isotropic even if all elements Q_{ij} are identical (then $\epsilon_Q = \delta_Q = 0$ and $g_Q = 1$). It is clear from equation D-6 that an additional condition required in this case is the absence of velocity anisotropy for P- and SV-waves ($\epsilon = \delta = 0$).

REFERENCES

Arts, R. J., and P. N. J. Rasolofosaon, 1992, Approximation of velocity and attenuation in general anisotropic rocks: 62nd Annual International Meeting, SEG, Expanded Abstracts, 640–643.

Ben-Menahem, A., and S. J. Singh, 1981, Seismic waves and sources: Springer-Verlag, New York.

Blangy, J. P., 1994, AVO in transversely isotropic media—An overview: Geophysics, **49**, 775–781.

Borcherdt, R. D., and L. Wennerberg, 1985, General P, type-I S, and type-II S waves in anelastic solids: Inhomogeneous wave fields in low-loss solids: Bulletin of the Seismological Society of America, **75**, 1729–1763.

Borcherdt, R. D., G. Glassmoyer, and L. Wennerberg, 1986, Influence of welded boundaries in anelastic media on energy flow, and characteristics of P, S-I, and S-II waves: Observational evidence for inhomogeneous body waves in low-loss solids: Journal of Geophysical Research, **91**, 11503–11518.

Carcione, J. M., 1997, Reflection and transmission of qP-qS plane waves at a plane boundary between viscoelastic transversely isotropic media: Geophysical Journal International, **129**, 669–680.

———, 2000, A model for seismic velocity and attenuation in petroleum source rocks: Geophysics, **65**, 1080–1092.

———, 2001, Wave fields in real media: Wave propagation in anisotropic, anelastic, and porous media: Pergamon Press.

Chichinina, T., V. Sabinin, and G. Ronquillo-Jarrillo, 2004, P-wave attenuation anisotropy for fracture characterization: Numerical modeling in reflection data: 74th Annual International Meeting, SEG, Expanded Abstracts, 143–146.

Gautam, K., M. Batzle, and R. Hofmann, 2003, Effect of fluids on attenuation of elastic waves: 73rd Annual International Meeting, SEG, Expanded Abstracts, 1592–1595.

Helbig, K., 1994, Foundations of anisotropy for exploration seismics: Pergamon Press.

Hosten, B., M. Deschamps, and B. R. Tittmann, 1987, Inhomogeneous wave generation and propagation in lossy anisotropic solids: Application to the characterization of viscoelastic composite materials: Journal of the Acoustical Society of America, **82**, 1763–1770.

Johnston, D. H., and M. N. Toksöz, 1981, Definitions and terminology, *in* O. H. Johnson and M. N. Toksöz, eds., Seismic wave attenuation: Geophysics reprint series 2, 1–5.

Krebes, E. S., and L. H. T. Le, 1994, Inhomogeneous plane waves and cylindrical waves in anisotropic anelastic media: Journal of Geophysical Research, **99**, 23899–23919.

Krebes, E. S., and M. A. Slawinski, 1991, On raytracing in an elastic–anelastic medium: Bulletin of the Seismological Society of America, **81**, 667–686.

Lynn, H. B., D. Campagna, K. M. Simon, and W. E. Beckham, 1999, Relationship of P-wave seismic attributes, azimuthal anisotropy, and commercial gas pay in 3-D P-wave multiazimuth data, Rulison field, Piceance basin, Colorado: Geophysics, **64**, 1293–1311.

Prasad, M., and A. Nur, 2003, Velocity and attenuation anisotropy in reservoir rocks: 73rd Annual International Meeting, SEG, Expanded Abstracts, 1652–1655.

Rathore, J. S., E. Fjaer, R. M. Holt, and L. Renlie, 1995, Acoustic anisotropy of a synthetic sandstone with controlled crack geometry: Geophysical Prospecting, **43**, 805–829.

Sayers, C. M., 1994, The elastic anisotropy of shales: Journal of Geophyical Research, **99**, no. B1, 767–774.

Tao, G., and M. S. King, 1990, Shear-wave velocity and Q anisotropy in rocks: A laboratory study: International Journal of Rock Mechanics and Mining Sciences and Geomechanics Abstracts, **27**, 353–361.

Thomsen, L., 1986, Weak elastic anisotropy: Geophysics, **51**, 1954–1966.

Tsvankin, I., 2001, Seismic signatures and analysis of reflection data in anisotropic media: Elsevier Science Publ. Co., Inc.

Tsvankin, I., and L. Thomsen, 1994, Nonhyperbolic reflection moveout in anisotropic media: Geophysics, **59**, 1290–1304.

Ursin, B., and A. Stovas, 2002, Reflection and transmission responses of a layered isotropic viscoelastic medium: Geophysics, **67**, 307–323.